Pharmacy Education (2023) 23(2) 200 - 206
https://doi.org/10.46542/pe.2023.232.200206

IAI SPECIAL EDITION

RESEARCH ARTICLE

Synthesis, molecular docking study, and *in vivo* biological evaluation of pyrazolopyridines derived from monocarbonyl curcumin analogues as potential anti-inflammatory agents

Enda Mora[1,2], Hilwan Yuda Teruna[2], Neni Frimayanti[1], Ihsan Ikhtiarudin[1], Noval Herfindo[1], Adel Zamri[2]

[1] Department of Pharmacy, Sekolah Tinggi Ilmu Farmasi Riau, Pekanbaru, Riau, Indonesia
[2] Department of Chemistry, Faculty of Mathematics and Sciences, Universitas Riau, Pekanbaru, Riau, Indonesia

Keywords
Anti-inflammatory
Docking
In vivo
Pyrazolopyridine
Synthesis

Correspondence
Hilwan Yuda Teruna
Department of Chemistry
Faculty of Mathematics and Sciences
Universitas Riau
Pekanbaru
Riau
Indonesia
hyteruna@lecturer.unri.ac.id

Abstract

Background: Pyrazolopyridines are heterocyclic compounds with nitrogen atoms in the ring and they have been used as one of the important pharmacophores in drug design. Pyrazole derivatives have been synthesised and applied in the pharmaceutical industry as active drugs. The recent commercial success of pyrazole COX-2 inhibitors has brought even more attention to the significance of this heterocyclic ring in medicinal chemistry. **Objective:** This study aimed to synthesise new compounds as anti-inflammatory candidates from the pyrazolopyridine group. **Method:** Synthesis was carried out using the Claisen-Schmidt reaction through condensation of substituted benzaldehyde and 4-piperidone to produce mono-ketone curcumin analogues, which were then cyclised with phenylhydrazine. The results of the synthesis were characterised using FT-IR, ^{1}H-NMR, and MS. Docking analysis was performed on the 3LN1 protein with MOE 2021.0901. Furthermore, an *in vivo* anti-inflammatory test was applied using a plethysmometer. **Results:** The synthesis results obtained two pyrazolopyridine compounds, and the docking results showed that both of these synthesised compounds could interact with the COX-2 receptor binding site. **Conclusion:** Compound **2** demonstrated good anti-inflammatory activities. This strategy is in the preliminary stages of identifying novel substances that may be used as anti-inflammatory agents in the future.

Introduction

Pyrazolopyridine plays an important role in the history of heterocyclic chemistry, and it has been used as an important pharmacophore and syntone active group in the field of organic chemistry and also in drug design (Bilavendran *et al.*, 2020; Secrieru *et al.*, 2020; Rashad *et al.*, 2014). Following the general concept of bioisosteres, as a typical synthetic form in medicinal chemistry, pyrazolopyridine has the potential to be manipulated in various ways to form new chemical structures and diverse bioactivities (Karrouchi *et al.*, 2018; El Gohary *et al.*, 2019; Giannouli *et al.*, 2020).

Pyrazolopyridine derivatives have been developed for some biological activities such as antimicrobial, anti-tumour, effects on the central nervous system (CNS), anti-inflammatory, antioxidant, and protein-inhibiting activity (El-Sayed *et al.*, 2021; Gomez *et al.*, 2021; Zhao *et al.*, 2019). In addition, drug frameworks approved by the Food and Drug Administration (FDA) in 2021, such as Asciminib as an allosteric tyrosine kinase BCR-ABL1 inhibitor, and *Vericiguat* (*Verquvo*) as a drug, was used to reduce the risk of cardiovascular death and heart failure (Mantzonidou *et al.*, 2021; Angeli *et al.*, 2022).

With this in mind, the authors synthesised several new pyrazolopyridine derivatives and conducted molecular docking studies of the compounds synthesised with the active site COX-2 (Protein database:3LN1) to predict their anti-inflammatory bioactivity.

Methods

Synthesis of pyrazolopyridine

The synthesis was conducted through two-step reactions, as described in Figure 1. Firstly, the synthesis of monocarbonyl curcumin analogue was carried out via Claisen-Schmidt condensation between N-benzylpiperidine-4-one with substituted benzaldehydes (2-chlorobenzaldehyde and 3,4,5-trimethoxybenzaldehyde). N-benzylpiperidine-4-one (5.0 mmol) and substituted benzaldehyde (10.0 mmol) were dissolved in absolute ethanol (20 mL), and potassium hydroxide solution (10%, 10.0 mL) was added into the mixture. Furthermore, the mixture was refluxed at 80°C, and the progress of the reaction was monitored by TLC analysis. After the reaction was completed, the mixture was neutralised by adding hydrochloric acid solution (10%) and cooled in a refrigerator for 24 h. The formed precipitate was filtered and washed with cold *n*-hexane and distilled water to yield the product (monoketone curcumin analogues). Secondly, the synthesis of pyrazolopyridine compound was performed via intermolecular cyclisation between the monoketone curcumin analogues and phenylhydrazine. Each of the monoketone curcumin analogue (2 mmol) and phenylhydrazine (4 mmol) was dissolved in absolute ethanol (10 mL), and sodium hydroxide solution (3N, 50 ml) was added to the mixture. Furthermore, the mixture was refluxed at 80°C, and the progress of the reaction was monitored by TLC analysis. After the reaction was finished, the mixture was poured on the crushed ice (30g) in an ice bath. The mixture was cooled in a refrigerator to afford the precipitate. The formed precipitate was filtered *in vacuo*, washed with distilled water and cold *n*-hexane and then dried at room temperature. Then both structures of the synthesised products were confirmed by spectroscopic analyses.

Molecular docking

The molecular structure of the ligands and celecoxib used as positive control were drawn using ChemDraw Professional 15.0; then, the 3D structure was further prepared using the Molecular Operating Environment (MOE) program 2020.0901 with MMFF94x force field and 0.0001 gradients. The molecular structure of the ligands is shown in Figure 2. The molecular structure of the protein (COX-2 enzyme) was downloaded from the rcsb.org site with PDB ID 3LN1. Then, using the MOE 2020.0901 software package, the protein molecular structure was created. The protein was then constructed using the parameter, i.e. RMS gradient was set to 0.01 kcal/mol/A, with CHARMM27 as the force field. Furthermore, the constructed structure is saved in PDB format so that it can later be used as a docking receptor.

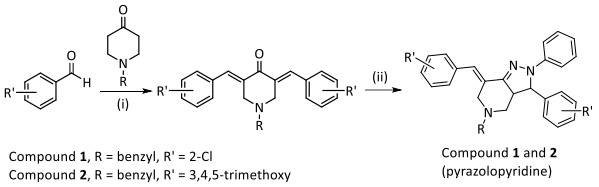

(i) = KOH, EtOH, 80°C, (ii) = Ph-NH-NH_2, NaOH, EtOH, 80°C

Figure 1: Synthesis route of pyrazolopyridine compounds

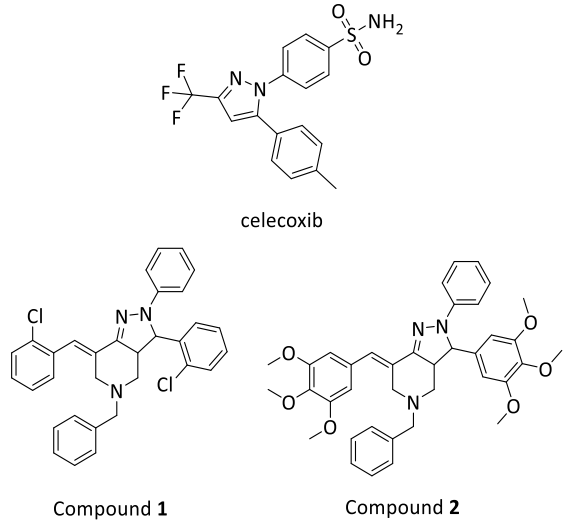

Figure 2: The 2D structures of ligands

Anti-inflammatory

This study was conducted after passing the ethical clearance released by the Ethics Unit of the Faculty of Medicine, University of Riau, document number: 13/150/U19.5.1.1.8/UEPKK/2022.

Carrageenan-induced paw oedema was used for the evaluation of in vivo anti-inflammatory activity of the synthesised compounds. Exactly 20 samples of live rats (Rattus novergicus) were divided into five groups consisting of four rats each. The first three were used for the anti-inflammatory dose test, and the remaining one as the test animal reserves. All groups were injected with carrageenan and left for one hour. Thereafter, the rats in the first group were only given 0.5% Na-CMC as a negative control, the rats in the

second group were given celecoxib 18 mg/kgBW as the positive control, and the rats in the third, fourth, and fifth were orally administered the synthetic compound mixed with Na-CMC, at a dose of 0.77 mg/kgBW; 1.54 mg/kgBW, and 3.08 mg/kgBW, respectively. The oedema volume was measured every 60 minutes with a plethysmometer for eight hours.

Results

Synthesis of pyrazolopyridine

*(E)-5-benzyl-7-(2-chlorobenzylidene)-3-(2-chlorophenyl)-2-phenyl-3,3a,4,5,6,7-hexahydro-2H-pyrazolo[4,3-c]pyridine (compound **1**)*

Compound 1 was obtained as a yellow crystal (33%) with a melting point (m.p) 151-152^{o}C. FTIR spectra (KBr, cm^{-1}): 3024 (C-H aromatic), 2890, 2806, 2752 (aliphatic C-H), 1596 (C=N), 1573, 1495, 1444 (aromatic C=C), 1305, 1120, 1030 (C-N), 763, 748 (C-Cl). ^{1}H NMR spectra (500 MHz, $CDCl_3$), δ (ppm): 7.62 (d, 1H, *J*=5 Hz), 7.42 (dd, 2H, *J*1=7.5 Hz, *J*2=1 Hz), 7.37 (s, 1H), 7.14-7.26, (m, 11H), 7.10 (d, 1H, *J*=5 Hz), 6.98 dd, 2H, *J*=10 Hz), 6.85 (t, 1H, *J*=7.5 Hz), 5.26 (d, 1H, *J*=10 Hz), 3.84 (d, 1H, *J*=15 Hz), 3.66 (d, 1H, *J*=15 Hz), 3.62 (d, 1H, *J*=15 Hz), 3.51 (dd, 1H, *J*1=10 Hz, *J*2=1 Hz), 3.38 (m, 1H), 3.12 (dd, 1H, *J*1=15 Hz, *J*2=5Hz), 2.65 (t, 1H, *J*=10 Hz). GC-MS: molecular ion and isotope peaks were found at m/z 524.1463 $[M+H]^+$ and m/z 526.1611 $[M+H+2]^+$, respectively.

(E)-5-benzyl-2-phenyl-7-(3,4,5-trimethoxy benzylidene)-3-(3,4,5-trimethoxyphenyl)-3,3a, 4,5,6,7-hexahydro-2H-pyrazolo[4,3-c]pyridine (*compound* **2**)

Compound 2 was obtained as a greenish-yellow crystal (84%), m.p. 148-149^{o}C. FTIR spectra (KBr, cm^{-1}): 3001 (aromatic C-H), 2931-2760 (aliphatic C-H), 1607 (C=N), 1596, 1511, 1496 (aromatic C=C), 1315, 1302 (C-N), 1255, 1247 (C-O), 1180, 1032 (C-N). ^{1}H NMR spectra (500 MHz, $CDCl_3$), δ (ppm): 7.26 (m, 6H), 7.20 (t, 2H, *J*=7.5 Hz), 7.10 (d, 2H, *J*=10 Hz), 6.88 (t, 1H, *J*=7.5 Hz), 6.61 (s, 2H), 6.45 (s, 2H), 4.50 (d, 1H, *J*=10 Hz), 4.10 (d, 1H, *J*=15 Hz), 3.87 (s, 3H), 3.86 (s, 3H), 3.84 (s, 6H), 3.78 (s, 6H), 3.75 (d, 1H, *J*=10 Hz), 3.62 (d, 1H, *J*=10 Hz), 3.37 (m, 1H), 3.29 (dd, 1H, *J* =10 Hz, 5 Hz), 3.12 (d, 1H, *J*=15 Hz), 2.54 (t, 1H, *J*=12.5 Hz). HRMS spectra: exact mass was calculated as $[M+H]^+$ = 636.3074 ($C_{38}H_{42}N_3O_6$) and molecular ion peak was found at m/z 636.3073.

Molecular docking

Molecular docking results showed that all two compounds (compounds 1 and 2) had excellent interactions with the protein. In this case, it was based on their binding factor, unfortunately not binding free energy. The results are presented in Table I, Figure 3 and Figure 4.

Table I: Docking results of celecoxib, compound 1 and compound 2

Compounds	S (kcal/mol)	RMSD	H bond	Hydrophobic	van der Waals	Other interactions	Binding factor
Re-docked Celecoxib	-11.93	0.90	Arg499	Phe504, Leu338, Arg106	-	Leu345, Ala513, Leu370, Gly512, Tyr371, Met508, Phe367, Trp373, Leu517, Val335, Val509, Ser516, Ile503, Tyr341, Gly340, Ser339, Gln178, His75, Ala502	23
Compound **1** (Pose 1)	-2,04	1,54	Arg106	Arg499	-	Tyr101, Leu78, Val74, Tyr341, His75, Gln178, Ala502, Phe504, Tyr371, Leu370, Ser339, Ile503, Leu338, Trp373, Val509, Met508, Gly512, Val335, Ala513, Ser516, Leu103, Leu345, Leu517, Val102, Met99	21
Compound **2** (Pose 4)	-1.19	1.49	-	Arg106, Arg499	Glu510	Ser105, Tyr101, Val102, Leu345, Ile331, Met99, Leu517, Leu520, Val335, Ser516, Leu370, Val509, Tyr371, Tyr334, Ala513, Trp373, Phe367, Ser339, Leu338, Met508, Ile503, Tyr341, Gly512, Phe504, Ala502, His75, Gln178, Pro71, Leu78, Val74	22

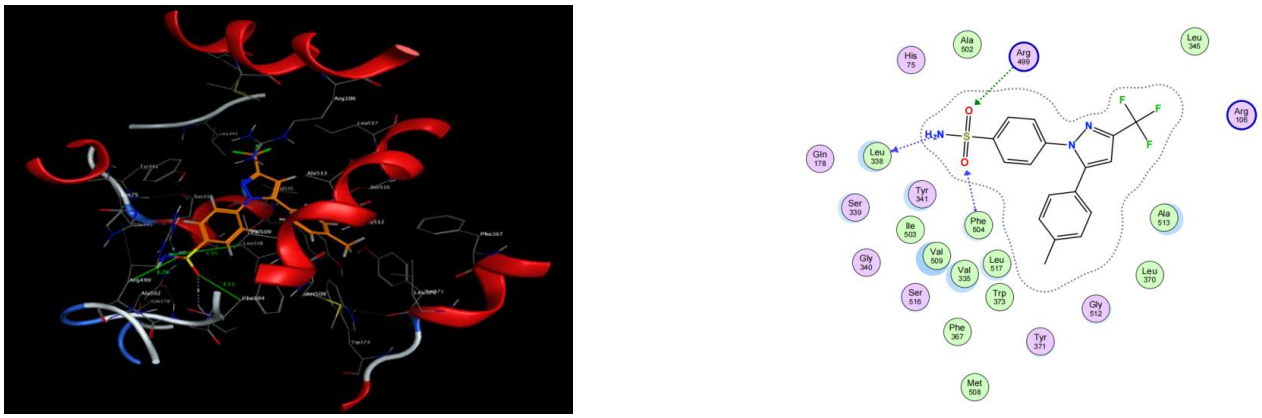

Figure 3: Spatial arrangement at the active site (3ln1.pdb) and celecoxib ligand interaction with protein

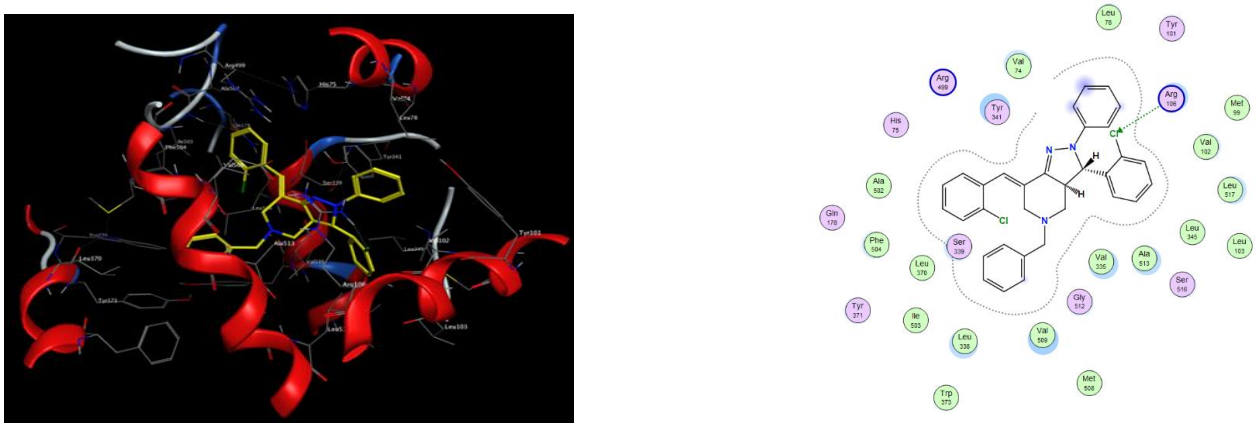

(a)

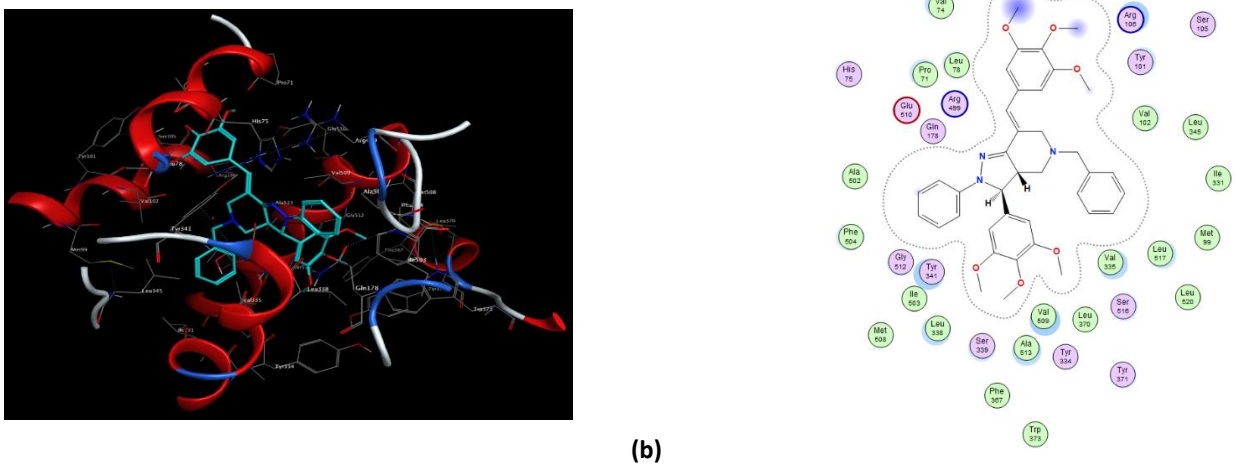

(b)

Figure 4: Spatial arrangement at the active site (3ln1.pdb), interaction of compound 1 (a) and compound 2 (b) with the protein, visualised using MOE 2021.0901 software

Anti-inflammatory

The anti-inflammatory test result showed that the two compounds have anti-inflammatory activity. Compound 1 with the chloro- substituent yielded 15.1% inhibition, and compound 2 with trimethoxy substitutions yielded 55.8% inhibition. The positive control (celecoxib) also showed 55.8% inhibition. 3,4,5-trimethoxy substituted compound responded with the same pattern of reducing oedema as seen in celecoxib, and as the best anti-inflammatory response in vivo. The results of the anti-inflammatory test are presented in Table II, Figure 5, and Figure 6. While the results of the anti-inflammatory test with a

plethysmometer showed a distinctive anti-inflammatory effect, observations through the anti-inflammatory graphs also revealed there was the same level of reduction in the oedema pattern of the celecoxib, the chloro- and methoxy- substituted compounds.

Table II: The result of *in vivo* anti-inflammatory test of compounds 1 and 2

Tested sample	Dosages (mg/Kg bw)	Oedema volume (mL) (Mean ± SD)								
		V0	V1	V2	V3	V4	V5	V6	V7	V8
Negative control (Na CMC)		0.95 ± 0.10	1.22 ± 0.06	1.23 ± 0.12	1.19 ± 0.18	1.48 ± 0.19	1.52 ± 0.28	1.50 ± 0.23	1.47 ± 0.21	1.41 ± 0.16
Positive control (Celecoxib)		0.90 ± 0.03	1.07 ± 0.12	1.22 ± 0.38	1.40 ± 0.32	1.33 ± 0.31	1.42 ± 0.34	1.46 ± 0.32	1.50 ± 0.30	1.48 ± 0.19
Compound 1	0.77	0.94 ± 0.08	1.22 ± 0.09	1.22 ± 0.10	1.26 ± 0.15	1.21 ± 0.15	1.23 ± 0.16	1.20 ± 0.13	1.18 ± 0.17	1.13 ± 0.14
	1.54	1.04 ± 0.07	1.26 ± 0.06	1.28 ± 0.08	1.23 ± 0.17	1.21 ± 0.09	1.20 ± 0.11	1.16 ± 0.11	1.13 ± 0.09	1.13 ± 0.10
	3.08	1.07 ± 0.10	1.51 ± 0.29	1.91 ± 0.34	2.05 ± 0.46	2.00 ± 0.42	1.96 ± 0.31	2.06 ± 0.53	1.98 ± 0.34	1.91 ± 0.28
Compound 2	0.77	0.82 ± 0.05	1.06 ± 0.23	1.31 ± 0.29	1.41 ± 0.37	1.43 ± 0.38	1.45 ± 0.45	1.47 ± 0.41	1.37 ± 0.36	1.36 ± 0.31
	1.54	0.86 ± 0.10	1.19 ± 0.10	1.23 ± 0.25	1.50 ± 0.15	1.45 ± 0.15	1.58 ± 0.23	1.59 ± 0.23	1.67 ± 0.27	1.59 ± 0.26
	3.08	0.86 ± 0.09	1.16 ± 0.18	1.22 ± 0.32	1.24 ± 0.32	1.26 ± 0.35	1.20 ± 0.38	1.23 ± 0.39	1.29 ± 0.39	1.29 ± 0.34

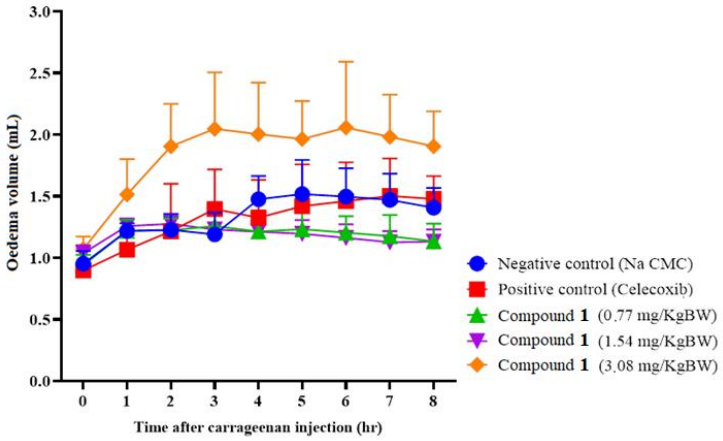

Figure 5: Oedema volume after administration of compound 1

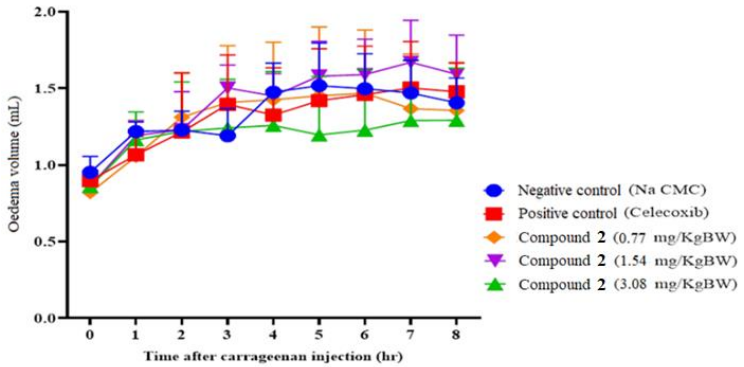

Figure 6: Oedema volume after administration of compound 2

Discussion

Pyrazolopyridine compounds were synthesised via two-step reactions. In the first step, the reaction mechanism began with the abstraction of alpha hydrogen of N-benzylpiperidine-4-one by hydroxide ion to form an enolate ion. The enolate ion acted as a nucleophile and attacked the electrophilic carbon of benzaldehydes to form new carbon-carbon (C-C) bonds, and *β*-hydroxy-ketone was formed as an intermediate, followed by dehydration to form the monocarbonyl curcumin analogues. In the second step, the hydrogen of phenylhydrazine was abstracted by a hydroxide ion to form a phenylhydrazine anion. This anion acted as a nucleophile and attacked both electrophilic carbons (*β*-carbon and carbonyl carbon) of curcumin analogues via the nucleophilic addition, followed by intermolecular cyclisation to form a pyrazolopyridine ring.

The presence of the pyrazolopyridine ring was confirmed by ^{1}H NMR spectra. The ^{1}H NMR spectra of both compounds showed some specific signals in the aliphatic region as described in the previous report (Ramalingam *et al.*, 2020). Compound 1 has 19 protons in the aromatic-olefinic regions and eight protons in the aliphatic region, whereas compound 2 only has 15 protons in the aromatic regions but showed more hydrogen (26 protons) in the aliphatic area due to the presence of six methoxy groups in the benzene aromatic rings. Overall, the results of the spectroscopic analyses of the synthesised compounds indicated conformity with the structure of the targeted compounds.

Through molecular docking, some parameters were obtained, including the Root Mean Square Deviation (RMSD). A more persistent association between the ligand and protein was suggested by a smaller binding free energy (Ramalingam, 2020). An indication of variations or faults while docking is the RMSD value. A lower RMSD value suggested that docking variations or errors were of a smaller magnitude. Based on the lowest binding free energy value and the lowest RMSD value, the best complex ligand-protein poses were selected. Both van der Waals interaction and hydrogen bonding were also employed as supporting parameters to determine the stability of complex ligand-receptor.

Based on the docking results, celecoxib, a positive control, had a binding free energy of -11.93 kcal/mol and RMSD of 0.90. Celecoxib interacted through the hydrogen bond with amino acid residues Arg499. Additionally, with Phe504, Leu338 and Arg106, this compound had hydrophobic interactions. The spatial arrangement of celecoxib with COX-2 is presented in Figure 3.

Compound 1 was determined to have a binding free energy value of -2.04 kcal/mol and an RMSD value of 1.54 as shown in Table I. It appears that the binding free energy of celecoxib had a higher negative value than compound 1. As a result, compound 1 had a longer time binding to the active site of COX-2. Based on the visualisation of the docking results, it was shown that compound 1 and the amino acid Arg106, formed a hydrogen bond. Additionally, this compound had hydrophobic interactions with Arg499. These interactions were used as parameters to determine the stability of the binding of the ligand to the receptor. The spatial arrangement of compound 1 with the protein is shown in Figure 4a.

Based on the docking results, compound 2 had a binding free energy of -1.19 kcal/mol and an RMSD value of 1.49 as shown in Table I. Compound 2 also had hydrophobic interactions with the same amino acids (Arg106 and Arg499). It also has a binding factor of 22. The spatial arrangement of compound 2 is depicted in Figure 4b. The Trimethoxy substitution in the structure of compound 2 can form more or stronger bonds with proteins or receptors (Ramalingam *et al.*, 2020).

Based on the docking results, the two compounds were tested for their anti-inflammatory activity. It was found that 3,4,5-trimethoxy substituted pyrazolopyridine had good docking results and also gave an inhibition of 55.85%, while the response and pattern of reducing oedema volume of compound 2 were better than compound 1. Based on the decrease in oedema volume, compound 2 had a decreasing pattern similar to that of the positive control, celecoxib. The average volume of oedema that appeared on the soles of the white male rats was lower than the negative control and positive control. Following the pattern of decline in the in vivo test, the synthesised pyrazolopyridine compound interacted with the COX-2 anti-inflammatory receptor. Furthermore, statistical analysis using one-way ANOVA analysis with the Duncan Multi Range test (DMRT) showed that there was a significant difference in the effect of oedema with other substituted pyrazolopyridine with a p-value of less than or equal to 0.05.

Conclusion

Two pyrazolopyridine compounds have been synthesised through a two-step reaction. The structures of the synthesised compounds matched the structures of the intended target molecules, according to the spectroscopic data produced by FT-IR, ^{1}H-NMR, and GC-MS or HRMS analyses. According to the in vivo study, compound 2 with 3,4,5-trimethoxy substituent

showed a good result as an active anti-inflammatory agent. This approach is in the early phases of finding novel substances that may be used as new candidates for anti-inflammatory agents in the future.

Acknowledgement

The authors thank DRTPM Universitas Riau for financial support through research contract No. 051/E5/PG.02.00.PT/2022.

References

Angeli, A., Kartsev, V., Petrou, A., Lichitsky, B. Komogortsev, A., Pinteala, M., Geronikaki, A. & Supuran, C.T. (2022). Pyrazolo[4,3-c]Pyridine Sulfonamides as Carbonic Anhydrase inhibitors: Synthesis, Biological and *In Silico* Studies, *Pharmaceuticals*, **15**(3):316. https://doi.org/10.3390/ph15030316

Bilavendran, J.D., Manikandan, A., Thangarasu, P. & Sivakumar, K. (2020), Synthesis and Discovery of pyrazolo-pyridine analogues as inflammation medication through pro- and inflammatory cytokine and COX-2 inhibition assessments. *Bioorganic chemistry*, **94**:103484. https://doi.org/10.1016/j.bioorg.2019.103484

El Gohary, N.S., Gabr, M.T. & Shaaban, M.I. (2019). Synthesis Molecular modelling and biological evaluation of new Pyrazolo[3,4-b]pyridine analogues as potential antimicrobial, anti-quorum-sensing and anticancer agents, *Bioorganic Chemistry,* **89**(2019):102976. https://doi.org/10.1016/j.bioorg.2019.102976

El-Sayed, R., Althagafi, I., Morad, M., El-Bahy, S.M. & El-Metwaly, N. (2021), synthesis and investigation of heterocyclic systems as pharmacological agents with conformational study and surface activity, *Journal of Molecular Structure*, **1240**:130597. https://doi.org/10.1016/j.molstruc.2021.130597

Giannouli, V., Lougiakis, N., Kostakis, I.K., Pouli, N., Marakos, P., Skaltsounis, A.L., Horne, D.A., Nam, S., Gioti, K. & Tenta, R. (2020), Design and Synthesis of New Substituted Pyrazolopyridines with Potent Antiproliferative Activity, *Medicinal Chemistry,* **16**(2):176–191. https://doi.org/10.2174/1573406415666190222130225

Gomez, A.A., Godoy, A. & Portilla, J. (2021), Functional Pyrazolo [1,5-a]pyrimidines: Current Approaches in Synthetic Transformations and Uses as an Antitumor Scaffold. *Molecules*, **26**(9):2708. https://doi.org/10.3390/molecules26092708

Karrouchi, K., Radi, S., Ramli, Y., Taoufik, J., Mabkhot, Y.N., Al-aizari, F.A. & Ansar, M. (2018), A Review: Synthesis and Pharmacological Activity of Pyrazole Derivatives: A Review, *Molecules,* **23**(1):134. https://doi.org/10.3390/molecules23010134

Mantzonidou, M., Pontiki, E. & Hadjipavlou-Litina, D. (2021), Pyrazole and Pyrazolines as Anti-Inflammatory Agents. *Molecule*s, **26**(11):3439. https://doi.org/10.3390/molecules26113439

Arulraj, R., Sivakumar, S., Suresh, S. & Anitha, K. (2020). Synthesis, vibrational spectra, DFT calculations, Hirshfeld surface analysis and molecular docking study of 3-chloro-3-methyl-2,6-diphenylpiperidin-4-one, *Spectrochimica Acta Part A: Molecular and Biomolecular Spectroscopy*, **232:**(118166). https://doi.org/10.1016/j.saa.2020.118166

Rashad, A.E., Shamroukh, A.H., Abdel-Megeid, R.E. & Ali, H.S. (2014). Synthesis and Isomerisation of Some Novel Pyrazolopyrimidine and Pyrazolotriazolopyrimidine Derivatives, *Molecules,* **19**(5):5459-5469. https://doi.org/10.3390/molecules19055459

Secrieru, A., O'Neill, P.M. & Cristiano, M.L.S. (2020). Revisiting the Structure and Chemistry of 3(5)-Substituted Pyrazole, *Molecules*, **25**(1): 42. https**://**doi.org/10.3390/molecules25010042

Zhao, Z., Dai, X., Li, C., Wang, X., Tian, J., Feng, Y., Xie. J., Ma, C., Nie, Z., Fan, P., Qian, M., He, X., Wu, S., Zhang, Y. & Zheng, X. (2019), Pyrazolon structural motif in medicinal chemistry: Retrospect and prospect, *European Journal of Medicinal Chemistry,* **186**:111893. https://doi.org/10.1016/j.ejmech.2019.111893